Journal of Hydrology 495 (2013) 13–22

Contents lists available at SciVerse ScienceDirect

Journal of Hydrology

journal homepage: www.elsevier.com/locate/jhydrol

Tree-ring reconstructed hydroclimate of the Upper Klamath basin

Steven B. Malevich *, Connie A. Woodhouse, David M. Meko

Laboratory of Tree-Ring Research, The University of Arizona, Tucson, AZ, United States

ARTICLE INFO

Article history:
Received 16 January 2013
Received in revised form 15 April 2013
Accepted 22 April 2013
Available online 9 May 2013
This manuscript was handled by Konstantine P. Georgakakos, Editor-in-Chief, with the assistance of Ashish Sharma, Associate Editor

Keywords:
Dendroclimatology
Drought
Klamath River
Water supply
Reconstruction
Precipitation

SUMMARY

This work presents the first tree-ring reconstructions of hydroclimate for the Upper Klamath River basin, which stretches from northern California into southern Oregon. The extended record provides a centuries-long perspective on the region's hydroclimatic variability and context for water-related political issues that have erupted in recent years. Reconstructions of water-year precipitation for Klamath Falls, Oregon (extending 1564–2004 and 1000–2010 CE) were developed to compare past drought severity with drought severity of the instrumental record (extending 1896–2011). The reconstructions suggest that variability exhibited during the instrumental period captures extremes of moderate-to-long-duration (6-, 10-, and 20-year) droughts, but not of short (single-year and 3-year) and very long (50-year) droughts, which were more severe during the 11th–13th centuries. The late-16th-century "mega drought" is present in the Klamath River basin, though with less strength than in the neighboring Sacramento River basin. Cool-season storm tracks appear to be a direct driver of hydroclimatic variability, leading to instances of see-saw like relationships with neighboring regions, such as in the mid-14th century. In contrast, the larger area of drought in the 12th century is suggestive of a long-term northward shift in cool-season storm tracks.

1. Introduction

The Klamath River basin is host to a wealth of biodiversity and human development. It has been the focus of heated discourse around water rights, resource allocation, and economic development (Levy, 2003; Service, 2003). These issues are linked to the Klamath River's natural hydroclimatic variability.

The basin is located in northern California and southern Oregon, in the transition zone of a cool-season precipitation dipole between the Pacific Northwest and Southwest US (Brown and Comrie, 2004). This dipole has been found to correspond to different phases of the El Niño/La Niña-Southern Oscillation (ENSO; Redmond and Koch, 1991; Cayan, 1996; Brown and Comrie, 2004). Consequently, the Klamath Basin has a variable relationship to dipole and ENSO phasing (Dettinger et al., 1998; Wise, 2010). Basin precipitation appears to have a strong relationship with Pacific/North American-like (PNA) patterns and Pacific cool-season storm track position (Wallace and Gutzler, 1981; Dettinger et al., 1998).

The drought of 2001–2002 is often cited as one of the worst droughts on record, throughout the western US. In the Klamath basin, snowpack and cumulative precipitation were 50% of average in January and February of 2001, with about 32% of normal cool-season precipitation (October, 2000–March, 2001) at Klamath Falls, Oregon (Risley et al., 2005; Braunworth et al., 2002). In the spring of 2001, the US Fish and Wildlife Service and the National Marine Fisheries Service issued opinions which noted a dramatic decline in local populations of endangered fish species over the past decades and recommended minimum levels in the Klamath River and Upper Klamath Lake (Service, 2003). As a result, the US Bureau of Reclamation reduced availability of water for irrigating agricultural lands in the Upper Klamath basin. Damages in 2001 from resulting agricultural losses in the surrounding communities were estimated at over $200 million (Levy, 2003). Tensions that followed saw the birth of an effort to negotiate differences between farmers, fishermen, environmentalists, and local tribes. The focus of this effort has been the development of a formal plan to manage the basin, and the launch of a river restoration project with the potential to become the largest such project in US history (US Department of the Interior, 2010).

Effective resource management requires understanding the range of variability possible in this natural system. Most water management decisions and planning are based on existing gauge records that extend, at best, into the early 20th century, and thus assume that the hydroclimatic variability exhibited over this time period is a fair representation of what may be expected in the future (e.g. Jain et al., 2002; Meko et al., 2012). One way to assess this assumption is to extend hydroclimatic records back in time using tree-ring data.

* Corresponding author. Address: Department of Geosciences, The University of Arizona, Tucson, AZ 85721-0058, United States. Tel.: +1 5202616765.
E-mail address: malevich@email.arizona.edu (S.B. Malevich).

0022-1694/$ - see front matter © 2013 Elsevier B.V. All rights reserved.
http://dx.doi.org/10.1016/j.jhydrol.2013.04.048

Tree-ring data have been used to reconstruct a variety of hydroclimatic variables, including streamflow, precipitation, salinity, drought, and snowpack (e.g. Stockton and Jacoby, 1976; Stahle et al., 2001; Woodhouse, 2003; Cook et al., 2004; Touchan et al., 2011). Reconstructions have been developed for the neighboring Columbia and Sacramento River basins (Earle and Fritts, 1986; Meko et al., 2001; Gedalof et al., 2004), but not yet for the Klamath basin. Previous dendrochronological work in the region includes the development of tree-ring chronologies from sites in northern California, southern Oregon, and the Klamath River basin (e.g. Meko et al., 2001; Stahle et al., 2001). Research indicates that the species *Juniperus occidentalis*, *Quercus douglasii*, *Pinus ponderosa*, and *Pinus jeffreyi*, are sensitive to cool-season moisture in this region (e.g., Meko et al., 2001, 2011). These tree species can achieve hundreds of years of age. Existing chronologies extend as far back as 530 CE (Table 1), with the incorporation of remnant material (dead wood on the landscape). These chronologies are useful for developing reconstructions of Klamath basin moisture variability. The drought of the 21st century can then be examined in light of a multi-century record of hydroclimatic variability.

This paper examines Upper Klamath basin hydroclimatic variability with reconstructions of Klamath basin precipitation. The droughts documented in the reconstructions are used to evaluate the representativeness of drought events in the instrumental record. Large scale implications of these reconstructions are then discussed, such as how long-term hydroclimatic variability in the Klamath basin fits within our larger understanding of western US hydroclimate.

Table 1
Tree-ring chronologies in predictor pools for reconstructions. Species codes (spp.): *Juniperus occidentalis* (JUOC), *Pinus ponderosa* (PIPO), *Pinus jeffreyi* (PIJE), and *Quercus douglasii* (QUDG). Period is the time coverage of site chronology after parsing and cropping such that a sample depth $\geqslant 5$. ITRDB sites annotated with "*" indicate sites recollected and updated for this study.

	Series	spp.	Period	ITRDB site
AGU	Arrow Gap Update	JUOC	530–2011	OR062*
ALU	Antelope Lake Update	PIPO	1493–2010	CA067*
BCC	Bear Creek Canyon	QUDG	1582–2004	CA648
BCU	Boles Creek Update	JUOC	1235–2010	CA629*
DIB	Dibble Creek	QUDG	1531–2004	CA652
DPR	Don Pedro Res. Update	QUDG	1564–2005	CA616
DRU	Dalton Reservoir Update	JUOC	1449–2010	CA065*
FBK	Frederick Butte Update	JUOC	936–2010	OR060*
FEA	Feather River Lake Oroville Update	QUDG	1585–2004	CA618
HRK	Horse Ridge Update	JUOC	1000–2010	OR061*
KAW	North Fork Kaweah River	QUDG	1503–2004	CA659
LCU	Lemon Canyon Update	PIJE	1535–2010	CA064*
LJK	Little Juniper Mt.	JUOC	1493–2010	OR018*
LTU	Log Cabin – Tioga Pass Update	PIJE	1422–2010	CA505*
LVU	Lakeview Update	PIPO	1560–2010	OR002*
PPP	Pacheco Pass State Park Update	QUDG	1549–2003	CA625
PUT	Putah Creek, Lake Berryessa	QUDG	1584–2004	CA663

2. Hydroclimatology of the Klamath River basin

The Klamath River drains a 40,795 km^2 basin and runs 423 km from its source in southern Oregon (elevation 1247 m), through northern California to the Pacific Ocean (Fig. 1). The Klamath River's total annual discharge (average 482 m^3 s^{-1}) is influenced by strong seasonal precipitation (Fig. 2), with peak discharge from January to March. Surface runoff from Upper Klamath cool-season precipitation is the primary source for Klamath River flow.

The main gage on the Upper Klamath River is at Keno, Oregon. The US Bureau of Reclamation has developed estimated natural streamflow at this gage, but the series extends to only 1949, leaving a relatively short period of overlap between tree-ring and natural flow gage data. There is some uncertainty regarding the estimated flow values due to the region's complex land use (US Bureau of Reclamation, 2004). Klamath Falls water-year (WY; October–September) precipitation is adopted as a proxy for Upper Klamath basin streamflow and hydroclimate because of these uncertainties in the flow record. The long Klamath Falls precipitation record is suitable for training and validating a reconstruction since precipitation in the Upper Klamath basin is the primary contributor to Klamath River flow and Klamath Falls precipitation is strongly and linearly related to flow (Fig. 3).

The atmospheric circulation pattern most closely associated with Klamath Falls precipitation is a mid-latitude wave train across the Northern Hemisphere (Fig. 4). This points to the importance of a cool-season PNA-like circulation pattern, guiding moisture from the Pacific across the region (Wallace and Gutzler, 1981). The PNA pattern guides and displaces cool-season jets and storms, and is a consistent control of interannual and decadal precipitation transport across the west coast of North America, especially in northern California and southern Oregon (Cayan, 1996; Dettinger et al., 1998; Abatzoglou, 2011). Klamath Falls WY precipitation is inversely correlated ($r = -0.38$, $n = 52$, $\alpha = 0.05$) with cool-season (November–April) 500 mb geopotential height anomalies off the northwest coast of North America, reflecting the influence of strong blocking ridges during cool-season droughts.

Klamath Falls WY precipitation shows no significant correlation with equatorial Pacific sea surface temperatures (SST; Fig. 4). This is not surprising given the Klamath Basin's transitional position between north and south ends of the ENSO precipitation dipole (Haston and Michaelsen, 1997; Cayan et al., 1998; Dettinger et al., 1998). Although there appears to be little direct and consistent association with ENSO variability, cool-season precipitation in this transition zone may be influenced by ENSO if the dipole boundary shifts north or south (Cayan et al., 1998; Dettinger et al., 1998; Brown and Comrie, 2004; Woodhouse et al., 2009; Wise, 2010).

3. Methods

3.1. Hydroclimatic reconstructions

The Klamath Falls WY-total precipitation record (http://cdiac.ornl.gov/epubs/ndp/ushcn/ushcn.html), which extends from WY 1896–2011, was selected as the target variable for reconstruction. A set of strategies was employed to develop a pool of candidate tree-ring chronology predictors for precipitation reconstruction. First, existing *Juniperus occidentalis*, *Pinus ponderosa*, *Pinus jeffreyi*, and *Quercus douglasii* chronologies from California and Oregon were obtained from the International Tree-Ring Databank (ITRDB; http://www.ncdc.noaa.gov/paleo/treering.html) and parsed. Initial screening excluded sites outside a 450 km buffer around the Klamath basin to emphasize chronologies related to Klamath basin climate variability directly, rather than through teleconnections. The network was not strictly delineated by the

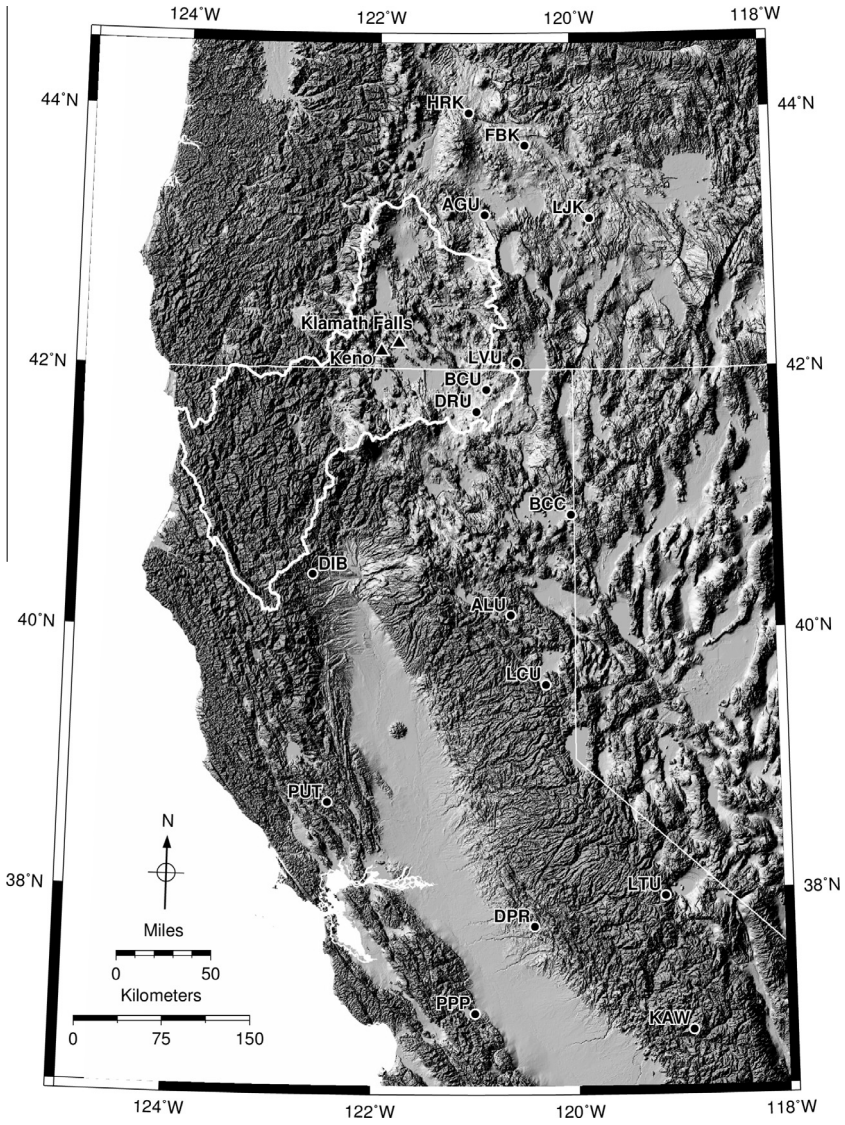

Fig. 1. Klamath River basin (white outline) and tree-ring chronology sites (circle) with Klamath Falls and Keno gauge (triangles).

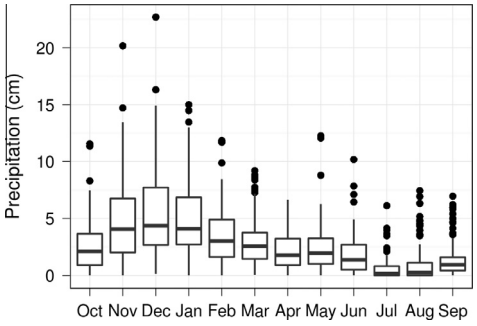

Fig. 2. Boxplots of monthly Klamath Falls precipitation (January 1895–December 2011). Note the dominant cool-season maximum.

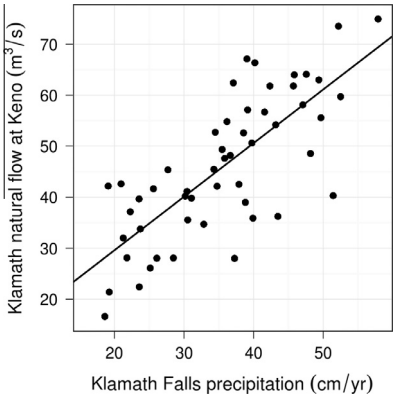

Fig. 3. Scatterplot of annual observations of Klamath River natural flow at Keno on Klamath Falls precipitation (1949–2000). R^2 for the fit linear model is 0.58.

physical basin boundaries as cool-season precipitation patterns important to streamflow typically extend beyond the spatial boundaries of individual river basins (Cayan, 1996).

The chronologies that passed the first level of screening were correlated with the Klamath Falls instrumental series. Chronologies without a statistically significant correlation ($\alpha = 0.05$) with the Klamath Falls instrumental series were removed, along with those that did not extend earlier then 1600. Ten chronologies from this candidate pool were selected for updating through field collection. The selection was guided by whether the site had (1) a strong

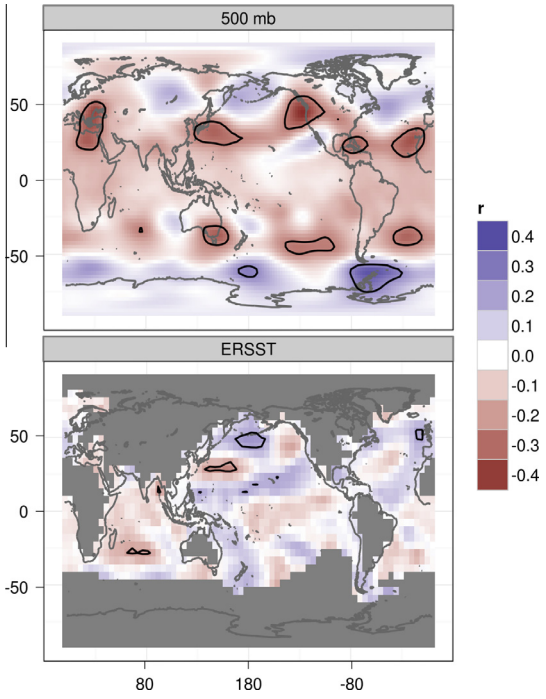

Fig. 4. Correlation field maps of WY Klamath Falls precipitation with (top) November–April mean NCEP/NCAR gridded 2.5° × 2.5° reanalysis 500 mb geopotential height (1949–2011; http://www.esrl.noaa.gov/psd/data/gridded/data.ncep.reanalysis.pressure.html) and (bottom) gridded 5.0° × 5.0° Kaplan extended reconstructed sea surface temperature (ERSST) anomalies (1896–2011; http://www.esrl.noaa.gov/psd/data/gridded/data.kaplan_sst.html), with the same 6 month period mean. Black contours indicate areas with statistically significant Pearson's *r* coefficient based on a Student's *t*-distribution test ($\alpha = 0.05$).

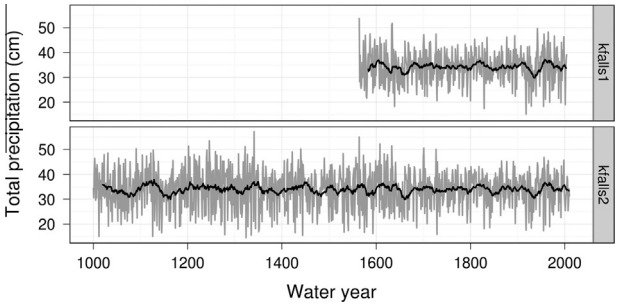

Fig. 5. The kfalls1 (1564–2004) and kfalls2 (1000–2010) reconstructions. Annual values are in gray and 20-year moving averages in black.

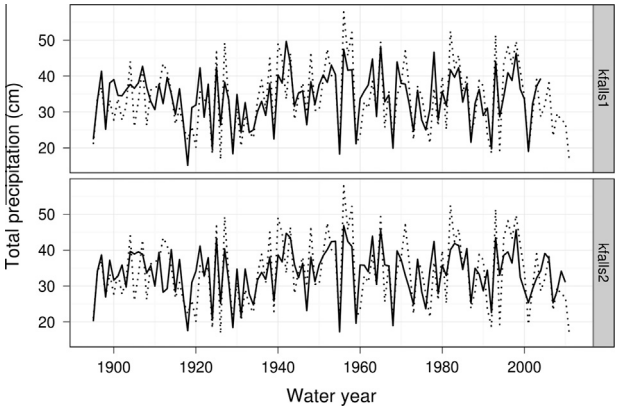

Fig. 6. Time plots of actual (dashed) and reconstructed Klamath Falls WY precipitation (solid) for their common period. Common period for kfalls1 is 1896–2004 and 1896–2010 for kfalls2.

Table 2
Performance statistics of reconstruction models. Training period is in water years. "No. Chrons" gives the number of tree-ring chronologies used by the reconstruction model. Other statistics defined in text.

Model	R^2_{adj}	$RMSE_{test}$ (cm)	*RE*	No. Chrons	Training period
kfalls1	0.59	6.31	0.54	7	1896–2003
kfalls2	0.53	6.47	0.50	3	1896–2010

correlation with precipitation and streamflow from the region, and; (2) adequate documentation to allow the original sampling site to be relocated. This strategy resulted in seventeen moisture-sensitive tree ring series for reconstruction (Table 1; Fig. 1).

Trees were sampled from the 10 sites selected for updating in October of 2010 and July of 2011. No less than twenty-five trees were sampled (two cores per tree) from each site. Samples were collected with an increment borer and processed using standard dendrochronological methods (Stokes and Smiley, 1996). Annual ring widths were cross-dated (Fritts, 2001) and measured with a Velmex measuring system. Quality control and chronology development were conducted using R (R Development Core Team, 2012) with the dplR package (Bunn, 2010) in addition to the COFECHA program (Holmes, 1983).

Measured tree-ring series from original and updated chronologies were detrended using a cubic smoothing spline (Cook and Peters 1981). Detrending is used to remove the age-related trend in ring widths believed to be primarily biological in origin (Fritts, 2001). In order to remove the age-related trend but retain multi-decadal scale information, we used a cubic spline with a 50% frequency-response cutoff at 67% the length of the measured series length (Cook et al., 1990). Both precipitation and detrended tree-ring series have significant autocorrelation. The detrended tree-ring series, however, have relatively higher orders of autocorrelation and account for a much larger proportion of the series' variance. Where statistically significant, the autoregressive component was therefore individually removed from the tree-ring series by "prewhitening" or fitting and filtering the series with an autoregressive model optimized to the Akaike Information Criterion (AIC; Akaike, 1974; Box et al., 1994). Tukey's biweight robust mean of the detrended and prewhitened series was then used as the site chronology (Cook and Kairiuksktis, 1990).

The following procedure was used to update existing chronologies with new samples. First, the core measurements from the original collection were obtained from the ITRDB, then detrended and prewhitened as described above. The 10 longest tree-ring width series from the original site collection were combined with the updated samples and processed into a preliminary site chronology. The common signal of a chronology, measured by the Expressed Population Signal (EPS; Wigley et al., 1984), was evaluated using a running 50-year window with 25-years of overlap between each window. Windows of this preliminary chronology with either an EPS below 0.85 (Wigley et al., 1984) or a sample depth below five trees, were then supplemented with additional tree-ring series from the original collection in order to reduce variance distortion from small sample size.

Klamath Falls precipitation was reconstructed using stepwise multiple linear regression with the predictor pool of seventeen tree-ring chronologies identified above. The model was fit using the full instrumental record and selected through backward selection with the objective of minimizing AIC (Burnham and Anderson, 2002). The full instrumental period was used for leave-one-out

Table 3
Klamath Falls instrumental record (1896–2011) *k*-year moving average ranks. Given years are water years and the last year in the *k*-year period. Units are cm.

Rank	1-Year	3-Year	6-Year	10-Year	20-Year	50-Year
1	16.13 (2011)	22.81 (1920)	24.73 (1934)	27.39 (1924)	28.37 (1934)	32.31 (1944)
2	16.79 (1926)	23.61 (2011)	25.29 (1920)	27.99 (1926)	28.70 (1935)	32.51 (1947)
3	18.31 (1924)	24.02 (1931)	26.32 (1933)	28.00 (1935)	29.01 (1933)	32.57 (1945)
4	18.62 (1992)	24.65 (1919)	26.79 (1921)	28.35 (1937)	29.09 (1936)	32.65 (1946)
5	19.10 (1955)	24.66 (1933)	26.85 (1935)	28.91 (1933)	29.35 (1937)	32.83 (1949)
6	19.25 (1994)	25.43 (1934)	26.98 (2011)	29.11 (1923)	29.85 (1932)	32.89 (1950)
7	19.28 (2001)	25.78 (1961)	27.10 (1922)	29.11 (2011)	30.33 (1939)	32.89 (1948)
8	20.19 (1920)	26.31 (1918)	27.83 (1919)	29.35 (1934)	30.49 (1938)	33.00 (1951)
9	20.42 (1931)	26.48 (1992)	28.06 (1924)	29.40 (1925)	30.57 (1931)	33.33 (1955)
10	20.47 (1929)	26.81 (1935)	28.13 (1936)	29.42 (2010)	31.39 (1930)	33.33 (1964)

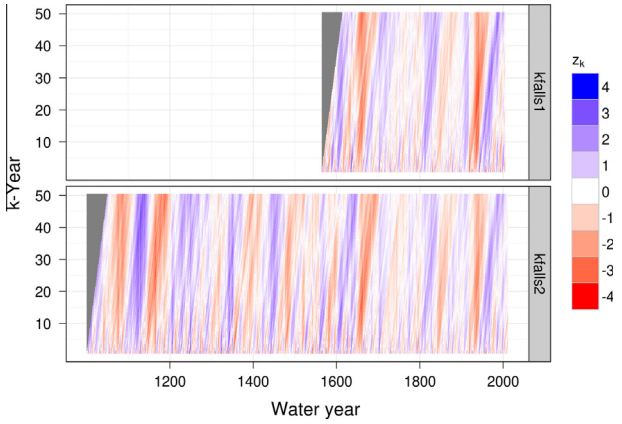

Fig. 7. Flame plots of kfalls1 (1564–2004) and kfalls2 (1000–2011) reconstructions summarizing moving average time series for 1- to 50-year moving average windows. Red colors indicate dry precipitation departures while blue colors show wet departures. Departures are measured relative to the reconstruction-mean. Window size, or number of years in moving average, plotted as *y*-axis. The plot's "flames" lean to the right of the plot because the moving average windows are right- and not center-aligned. The color values are *z*-scores independently scaled to each *k*-year moving average series. (For interpretation of the references to color in this figure legend, the reader is referred to the web version of this article.)

cross-validation so that extreme drought events at the beginning and end of the record could be used to test and train the model. Two validation statistics, the root mean squared error (RMSE) and reduction of error (RE), were calculated (Fritts et al., 1990).

RMSE is given by:

$$\mathrm{RMSE} = \sqrt{\frac{\mathrm{SSR}_{test}}{n}}$$

where SSR_{test} is the sum of squared residuals for the test observations during cross-validation and n is sample size of predictand. RE is given by:

$$\mathrm{RE} = 1 - \frac{\mathrm{SSR}_{test}}{\sum_{i=1}^{n}(y_i - \bar{y})^2}$$

where y_i is ith observation and $\bar{y}$ is the calibration-period arithmetic mean of the predictand. The statistic RE, ranging from $-\infty$ to 1.0, measures the model's error variance relative to the variance of the predictand around its calibration mean. An RE of 1.0 reflects perfect model performance in validation, while an RE greater than zero is considered evidence of some validation skill (Fritts et al., 1990).

Two models were created using the above method. One model, "kfalls1", was trained using the entire available pool of chronology predictors, whose common time period is 1600–2003. A second model, "kfalls2", was trained with three chronologies whose common period is 1000–2010. In this manner, one model emphasizes predictive performance (larger and presumably more robust predictor set) while the other model emphasizes length of reconstruction.

3.2. Drought analysis

Drought and hydroclimatic variability were identified and assessed using a moving average/Monte Carlo-based method originally described by Touchan (1999) and Meko et al. (2001). The analysis was conducted with $j = 1000$ iterations. For the ith iteration, a random noise vector, $\boldsymbol{\epsilon}_i$, the same length as the reconstruction, was formed by drawing from a $N(0, RMSE^2)$ distribution, and was added to time series, $\hat{\mathbf{y}}$, the reconstructed precipitation. The resulting ensemble of j noise-added reconstructions is a set of plausible precipitation realizations given the single reconstruction and its uncertainty as estimated from the validation process. An empirical confidence interval for any statistic derived from the reconstruction can be estimated from the empirical frequency distribution (CDF) of that statistic for the j ensemble members. One such statistic is the minimum k-year moving average of annual precipitation. Ranked 3-, 6-, 10-, 20- and 50-year moving averages were used to measure severity of short and long drought periods in the reconstruction and instrumental series. The empirical distribu-

Table 4
The kfalls1 reconstruction (1564–2004) *k*-year moving average ranks. Remainder of caption as in Table 3.

Rank	1-Year	3-Year	6-Year	10-Year	20-Year	50-Year
1	15.14 (1918)	24.22 (1919)	26.57 (1934)	28.49 (1937)	29.80 (1936)	32.37 (1660)
2	17.44 (1829)	24.36 (1581)	27.96 (1933)	28.76 (1935)	29.93 (1934)	32.39 (1661)
3	18.29 (1955)	25.84 (1931)	28.21 (1936)	28.94 (1938)	29.93 (1937)	32.41 (1659)
4	18.29 (1639)	25.96 (1918)	28.34 (1992)	29.32 (1660)	29.97 (1935)	32.61 (1658)
5	18.38 (1929)	26.11 (1920)	28.40 (1920)	29.35 (1939)	30.43 (1933)	32.61 (1662)
6	19.04 (2001)	26.46 (1569)	28.53 (1935)	29.42 (1936)	30.63 (1939)	32.68 (1667)
7	19.68 (1924)	26.48 (1935)	28.90 (1919)	29.43 (1653)	30.84 (1941)	32.70 (1663)
8	19.70 (1992)	26.61 (1992)	28.92 (1631)	29.46 (1933)	30.95 (1660)	32.82 (1664)
9	19.94 (1968)	26.68 (1595)	28.99 (1660)	29.86 (1924)	31.05 (1940)	32.82 (1655)
10	20.52 (1729)	26.77 (1794)	29.00 (1937)	29.90 (1940)	31.07 (1938)	32.85 (1656)

Table 5
The kfalls2 reconstruction (1000–2010) *k*-year moving average ranks. Remainder of caption as in Table 3.

Rank	1-Year	3-Year	6-Year	10-Year	20-Year	50-Year
1	14.49 (1324)	21.67 (1273)	26.05 (1356)	27.67 (1660)	29.80 (1661)	31.83 (1189)
2	14.99 (1012)	21.89 (1353)	26.62 (1580)	28.51 (1149)	29.88 (1660)	31.92 (1188)
3	15.00 (1126)	23.24 (1580)	26.97 (1934)	28.66 (1483)	29.89 (1662)	31.93 (1187)
4	15.42 (1444)	23.51 (1185)	27.04 (1145)	28.73 (1658)	29.91 (1164)	32.01 (1086)
5	15.49 (1335)	23.80 (1595)	27.05 (1660)	28.77 (1659)	30.16 (1159)	32.03 (1179)
6	15.67 (1279)	24.01 (1146)	27.31 (1355)	28.88 (1655)	30.35 (1163)	32.06 (1185)
7	15.83 (1729)	24.06 (1795)	27.34 (1480)	28.88 (1148)	30.36 (1663)	32.06 (1184)
8	16.17 (1593)	24.32 (1354)	27.85 (1518)	28.92 (1164)	30.41 (1667)	32.10 (1190)
9	16.48 (1145)	24.75 (1581)	27.94 (1146)	28.92 (1657)	30.42 (1936)	32.11 (1083)
10	16.51 (1428)	24.78 (1083)	28.02 (1273)	29.01 (1935)	30.43 (1934)	32.17 (1178)

Table 6
Lowest *k*-year moving averages of observed and reconstructed annual precipitation. Time coverage is 1896-2011 for observed series (*inst*), 1564–2004 for the short reconstruction (*kfalls1*), and 1000–2010 for the long reconstruction (*kfalls2*). Entries for *kfalls1* are not included unless the lowest value is found outside of the instrumental period. Probability, *P*, is the Monte Carlo derived probability that the actual (unknown) precipitation in the driest reconstructed year or period was lower than the observed minimum in the instrumental record. Empirical distributions which serve as the basis for these probabilities can be found in Fig. 8. Listed years are water years and the last year in the *k*-year period. Precipitation units are cm.

k-Year	*inst*	*kfalls1*	*P*(*kfalls*1 < *inst*)	*kfalls2*	*P*(*kfalls2* < *inst*)
1	16.13 (2011)	–	–	14.49 (1324)	0.58
3	22.81 (1920)	–	–	21.67 (1273)	0.62
6	24.73 (1934)	–	–	26.05 (1356)	0.27
10	27.39 (1924)	–	–	27.67 (1660)	0.38
20	28.37 (1934)	–	–	29.80 (1661)	0.11
50	32.31 (1944)	32.37 (1660)	0.45	31.83 (1189)	0.61

tion function of lowest *k*-year moving average for the *j* noise-added reconstructions was then applied to estimate long-term non-exceedance probability of the lowest *k*-year moving average in the instrumental record.

4. Results and discussion

4.1. Reconstructions of Klamath Falls precipitation

Performance statistics for the two Klamath Falls precipitation reconstruction models underscore the strong precipitation signal in the tree-ring chronologies (Table 2). The kfalls1 model explains 61% of the variance in the training set and the kfalls2 model explains 54%. The kfalls1 model uses seven chronologies (AGU, DIB, DPR, FBK, LCU, LTU, and LVU) and yields a reconstruction interval of 1564–2004. The kfalls2 model relies on just three chronologies (AGU, FBK, and HRK), but more than doubles the extent of the reconstruction interval to 1000–2010 (Fig. 5).

Analysis of residuals for both reconstruction models shows no grave violations of linear regression assumptions. Model residuals are approximately normally distributed, homoscedastic, and not significantly autocorrelated. Relationships between variables show no strong evidence of nonlinearity. Agreement of observed and reconstructed precipitation (by both models) for the instrumental period is shown by the time series plots in Fig. 6. In general, kfalls1 and kfalls2 behave similarly over their shared period ($r = 0.88$). The magnitude of some wet events is underestimated, as seen in the late 1950s and early 1980s. The magnitude of several short dry events is also not fully realized in the models, most notably 1926, 1992, and 1994. Both models have validation skill, as reflected by the high RE values (Table 2).

4.2. Drought analysis results

The most notable droughts in the instrumental record occur over the period from 1910 to 1940. The list of lowest 10 values for 6-, 10-, 20-, and 50-year moving averages is dominated by periods in or overlapping 1910–1940 (Table 3). The lowest single-year and 3-year events have increasing representation from outside this interval, though the early 20th century continues to dominate. Notable recent dry events include: 2011 (a single year exclusive to the instrumental record), 1959–1961, 1990–1992, 1992, 1955, 1994, and 2001.

The kfalls1 reconstruction places the droughts of the instrumental period in the context of the past four centuries. Several sustained periods of drought are evident in kfalls1, including a period of considerable drought in the 1600s, that rivals the severity of the early 20th century drought (Fig. 7). The late 17th century appears to dominate the driest 50-year moving averages (Table 4). The lowest 10- and 20-year moving averages of the early 20th century are similar in magnitude to those of the mid- to late-17th century. The lowest ranking 3-year averages on kfalls1 occur in the late 1700s (3-year period ending in 1794) and the late 16th century (3-year periods ending in 1569, 1581 and 1595). The 20th century is strongly represented in the single-year ranks. The reconstruction brings new single-year events into the top driest events: 1829, 1639, and 1729. The second lowest single year of the instrumental period by the observed precipitation data, 1926, was not fully captured by either reconstruction, but is reconstructed as the sixteenth driest single year in kfalls1 and 147th in kfalls2. But, 1926 still ranks as a relatively dry reconstructed year: 14.5 percentile of kfalls2, and 12.4 percentile of kfalls1. The 21st century does contain one of the driest 10 years (2001) in the kfalls1 reconstruction (as well as the driest year in the entire instrumental record, 2011, which is outside the time coverage of the reconstructions).

The kfalls2 reconstruction, which begins in 1000 CE, extends the temporal window for historical droughts far beyond the window provided by kfalls1 (Figs. 5 and 7). It is apparent from kfalls2 that droughts more persistent and severe than those of the 20th century have likely occurred over the course of the past millennia. The list of lowest 20- and 50-year moving averages shows that the 11th and late 12th centuries contain periods drier than any in the early 20th century (Table 5). The period prior to the start

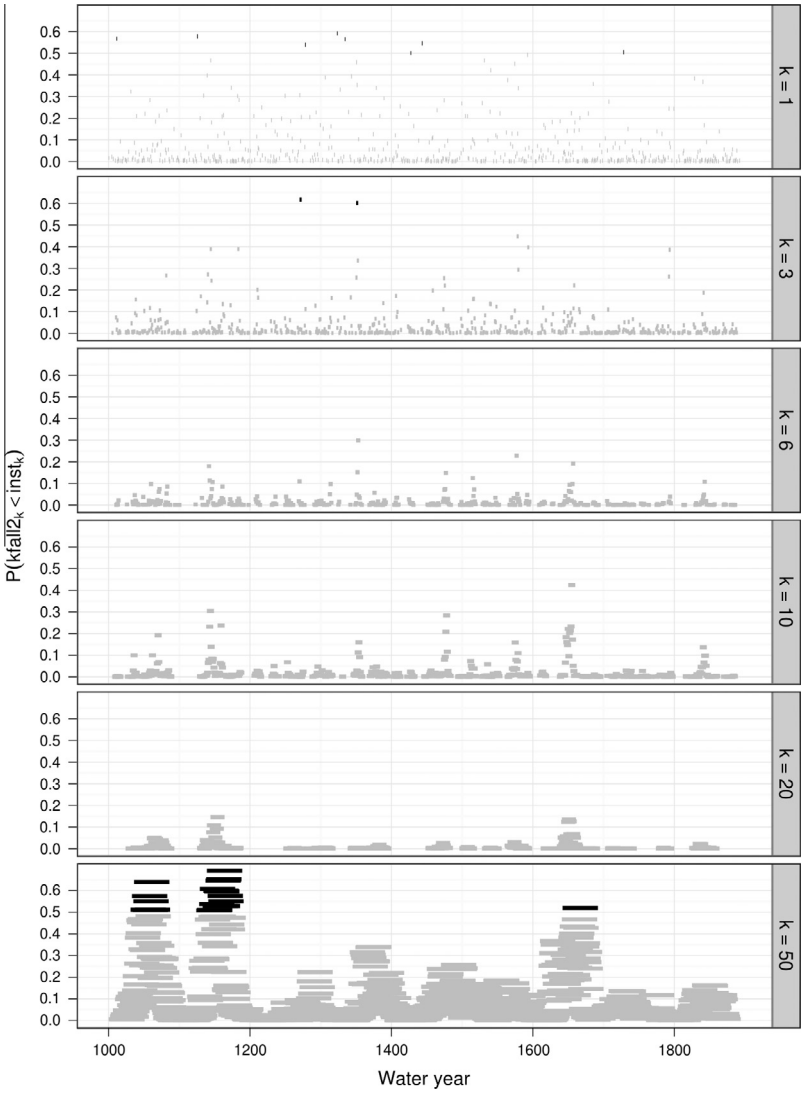

Fig. 8. Estimated probability that the actual precipitation for a given *k*-year moving average segment of the tree-ring record was lower than the lowest *k*-year moving average value from the instrumental record. Segments with an estimated probability above 0.5 are highlighted black. Those below 0.5 are gray. Probabilities are derived from noise-added reconstructions (see text). Listing of the single lowest values for each *k*-year moving averages from both kfalls1 and kfalls2 can be found in Table 6.

of the 17th century dominates the list of lowest single-year and 3-year moving averages in kfalls2: only 3-year events ending in 1729 and 1795 fall outside this period. The dry events of the 1600s noted in the kfalls1 reconstruction are also present in the kfall2 reconstruction's 10- and 20-year moving averages.

The Monte Carlo noise-added reconstructions give the empirical probability that the lowest precipitation event (annual-total or *k*-year moving average) in the reconstructed period was lower than the lowest observed precipitation in the instrumental period. Results show that the kfalls1 reconstruction flags no past drought back to 1564 CE with more than an even probability ($p = 0.50$) of being more severe than the most severe drought of the instrumental period (Table 6). Model kfalls2's extension to 1000 CE, on the other hand, indicates that single-year, 3-year, and 50-year moving averages lower than any encountered in the instrumental period probably ($p > 0.50$) occurred in the distant past, especially during the medieval period (Fig. 8). The noise-added reconstructions indicate a 58% probability that the actual precipitation in 1324 ($\hat{y} = 14.49$ cm) was lower than the record low observed precipitation (16.13 cm, 2011). Likewise, the probability is 62% that 3-year moving average precipitation in 1271–1273 ($\hat{y} = 21.67$ cm), was lower than the instrumental record's lowest 3-year average (22.81 cm, 1918–1920). Finally, the probability is 61% that the 50-year moving average in 1140–1189 ($\hat{y} = 31.83$ cm) was lower than the instrumental record's lowest 50-year moving average (32.31 cm, 1896–1944). Probabilities are relatively low (below 50%) – though non-zero – that 6-, 10-, and 20-year moving averages of actual precipitation lower than any in the instrumental period may have been encountered in the reconstruction.

4.3. Klamath basin droughts in regional context

The droughts documented in Klamath basin are often widespread throughout regions of western North American. By comparing these events with those documented by other hydroclimatic reconstructions, it is possible to examine the spatial nature and extent of notable dry periods. The severity of intermediate-duration droughts of the early 20th century found in Klamath basin have also been noted in reconstructions of the Sacramento River (Earle, 1993; Meko et al., 2001), Columbia River (Gedalof et al., 2004), and Upper Yellowstone River (Graumlich et al., 2003). This period is noted for a marked dipole between low snowpack in the Northern

Rockies and Greater Yellowstone region, and high snowpack in the watersheds of Wyoming and Colorado (Pederson et al., 2011).

Other well-known periods of severe and widespread drought are the late 16th century and the medieval period droughts (e.g., Stahle et al., 2000; Cook et al., 2004; Meko et al., 2007). The Sacramento River reconstruction (Meko et al., 2001) shares a number of similarities with the Klamath basin during these droughts as well as some differences. It should be noted that both the Klamath and Sacramento reconstructions share many of the same chronologies as predictors, so similarities may be inflated. However, the correlation between the instrumental record for Sacramento River streamflow and Klamath Falls precipitation are virtually the same as the correlation between the reconstructed series, suggesting inflation is not an important issue (instrumental records, $r = 0.62$; kfalls1 and kfalls2 reconstructions, $r = 0.64$, $n = 72$, $\alpha = 0.05$). There are differences between the reconstructions that may be related to regional climatology. The late 1500s "mega drought" in western North American (Stahle et al., 2000) is a joint-drought event between the reconstructed Sacramento and Upper Colorado River basin records (Meko and Woodhouse, 2005), and contains the lowest single-year and 3-year moving average flows in the Sacramento reconstruction. This study's reconstructions imply a different drought response for the Klamath basin. The Klamath basin reconstructions suggest it is unlikely that the late-1500s mega drought produced dry events more severe than any in the instrumental period. Tree-ring chronologies show that while southern Oregon and northern California largely exhibit an expected low-growth anomaly during this late 1500s event, a portion of these chronologies along the California-Oregon border show positive or neutral growth anomalies for portions of this dry period (Meko and Woodhouse, 2005). In addition, a network of snowpack reconstructions for this period suggests decadal-scale antiphasing between portions of the northwestern US (average and above average snowpack) and the Upper Colorado River basin (below average snowpack) (Pederson et al., 2011). This indicates that the Klamath basin may have been on the wet edge of the boundary between non-drought conditions in the Pacific Northwest and drought conditions across regions to the south and east.

In the 1350s, the Sacramento River flows switch abruptly from high to low flows, while in the southern Sierra Nevada and White Mountains of California, a change from dry to wet conditions is documented (Graumlich, 1993; Stine, 1994; Hughes and Funkhouser, 1998; Meko et al., 2001). The transition from wet to dry is also present in the kfalls2 reconstruction. In contrast to the late 16th century drought, the Klamath appears to part of a region that includes the Sacramento River basin that behaves in opposition to regions to the south. This regional pattern of dry–wet contrast is indicative of a shift of wintertime jet stream-driven storm tracks (Dettinger et al., 1998; Meko et al., 2001).

The mid-1100s drought is well-documented throughout western North America (e.g., Cook et al., 2004). In the Klamath basin, this period contains the lowest 50-year moving average value in the last millennium. In the Upper Colorado River reconstruction (Meko et al., 2007) the mid-1100s is a more extreme dry event than the late 16th century drought (Meko et al., 2012). In the Sacramento River reconstruction it is the second most severe 20-year average event (Meko et al., 2001, 2012). This large moisture deficit is also found in precipitation reconstructions in the Colorado Plateau (Salzer and Kipfmueller, 2005) and Great Basin (Hughes and Funkhouser, 1998). Temperature and precipitation reconstructions in the Sierra Nevada of southern California have identified this period as the warmest 20-year period and fourth driest period in the 1000-year long reconstruction (Graumlich, 1993). Given the severity of this drought in the Klamath reconstruction and the widespread nature of this drought across the western US, this is evidence that this mid-1100s drought is linked with a persistent northward shift in winter storm tracks (Stine, 1994; Meko et al., 2007).

5. Summary and conclusion

This paper presents the first tree-ring reconstructions of Upper Klamath basin hydroclimate, and examines how well the instrumental record represents the full range of natural hydroclimatic variability, and especially of drought. Results indicate that the Klamath Falls instrumental record (1896–2011) probably represents 1000-year extremes of drought on timescales of 6- to 20-years, but not on shorter and longer timescales. The lowest reconstructed moving averages of length 6, 10 and 20 years in the entire reconstruction spanning 1000–2010 occurred from the late 1910s to the late 1930s. The dryness of the early 20th century in the Klamath basin in a long-term context is consistent with other paleoclimatic reconstruction in the surrounding region (Earle, 1993; Meko et al., 2001; Gedalof et al., 2004; Graumlich et al., 2003).

Outside intermediate timescales (6–20 years), the instrumental record appears to be less representative of extreme drought conditions in the Klamath basin. The driest single years and the lowest running means of length 3, 5, and 50 years are found in the mid-1600s and the medieval period. The relative severity of drought in 1000s and 1100s in the Klamath basin is consistent with an expanded spatial area of drought over the western United States from 900 to 1300, as inferred from a continental network of tree-ring reconstructed Palmer Drought Severity Index (PDSI) (Cook et al., 2004). The late 1500s "mega drought", strongly present in the Upper Colorado River and the Sacramento River basins (Meko and Woodhouse, 2005), leaves a less prominent trace in the tree-ring record of the Klamath.

It should be noted that events prior to 1564, the period with the most severe and persistent drought, are based on the reconstruction model with only three chronologies. These three moisture-sensitive *Juniperus occidentalis* chronologies have played a key role in previous streamflow studies which have also incorporated tree-ring records of extremely moisture-sensitive *Quercus douglasii* chronologies (e.g. Meko et al., 2001). There are gains in performance from models kfalls2 to kfalls1 that reflect the strong drought signal of Q*uercus douglasii*, but the length of *Quercus douglasii* chronologies in the region are restricted to roughly the past 500 years, limiting reconstruction length. The unusually prolonged droughts of the medieval period underscores the importance for hydroclimate studies to balance optimal model performance with the need to cover drought periods that predate the best moisture-sensitive tree-ring chronologies. Additional field collections of tree-ring data would likely improve the Klamath reconstructions by strengthening the hydroclimatic signal in the tree-ring network and reducing reconstruction uncertainty. Updated or new collections would also provide direct long-term tree-ring context for the recent year, 2011, the driest single year in the Klamath Falls precipitation record. Updating tree-ring chronologies would ensure this key year is part of the calibration period, and allow a comparison of this most recent dry event with the events of the medieval period.

Klamath basin hydroclimatic variability is associated with interannual and decadal blocking circulation patterns in the eastern North Pacific (Dettinger et al., 1998). Because of this, the Klamath basin reconstruction, used in concert with other reconstructions, may be used to identify western United States drought events linked with storm-track shifts. The dry/wet shift of states in the mid-1300s may well be associated with a southward storm-track shift. The 1100s may be another such case, with a possible northward shift in cool-season storms. Future hydrocli-

matic reconstructions which extend to this event, especially if these are located north of the Klamath basin, would help to further test this hypothesis. Another important factor, Pacific SST variability, also plays a role in the spatial patterns of cool-season precipitation across the western US, influencing the precipitation dipole. Although the Klamath basin is in a transitional region with respect to the dipole (Dettinger et al., 1998; Wise, 2010), the dipole boundary is dynamic. If it is assumed that the western United States precipitation dipole dynamic exists throughout the length of the reconstruction, it may be useful to use the Klamath basin reconstruction as an indicator for the location of the dipole boundary. For example, a sustained wet period in the Klamath basin, coinciding with similar conditions in a northern, wet portion of the dipole could indicate the dipole boundary has migrated south to include the Klamath basin in the northwest US end of the dipole.

Efforts to manage water-supply on the Klamath River basin may benefit by considering the early 20th century drought, particular when assessing the impact of moderate-length drought events. However, single-year, 3-year, and longer 50-year events are best represented by the longer kfalls2 reconstruction. These reconstructed drought events may be helpful as possible scenarios when examining the impact of drought on reservoirs and water allocations. The drought events of the past decade have had economic and political impact. If sustained dry events such those which appear in the early 20th century, 1000s, or 1100s were to be experienced today, it would prove a challenge to those who manage or draw on Klamath basin water supplies.

Acknowledgements

Special thanks to Dr. Andrew Comrie for input and review, Holly Faulstich and Mark Losleben for help with field work, and John Danloe for lab assistance. Thanks also to the comments from two anonymous reviewers. This research is funded by a research grant from the California Department of Water Resources (4600008850) and a WaterSmart grant from the US Bureau of Reclamation (R11AP81457).

References

Abatzoglou, J.T., 2011. Influence of the PNA on declining mountain snowpack in the Western United States. Int. J. Climatol 31 (8), 1135–1142.
Akaike, H., 1974. A new look at the statistical model identification. IEEE Trans. Autom. Control 19 (6), 716–723.
Box, G., Jenkins, G.M., Reinsel, G., 1994. Time Series Analysis: Forecasting and Control. Prentice Hall.
Braunworth, W.S., Welch, T., Hathaway, R., 2002. Water Allocation in the Klamath Reclamation Project, 2001: An Assessment of Natural Resource, Economic, Social and Institutional Issues with a Focus on the Upper Klamath Basin, Oregon State University Extension Service.
Brown, D.P., Comrie, A.C., 2004. A winter precipitation 'dipole' in the western United States associated with multidecadal ENSO variability. Geophys. Res. Lett., 31(9), L09203.
Bunn, A.G., 2010. Statistical and visual crossdating in R using the dplR library. Dendrochronologia 28 (4), 251–258.
Burnham, K., Anderson, D., 2002. Model Selection and Multimodel Inference, second ed. Springer, New York.
Cayan, D.R., 1996. Interannual climate variability and snowpack in the Western United States. J. Climatol. 9 (5), 928–948.
Cayan, D.R., Dettinger, M.D., Diaz, H.F., Graham, N.E., 1998. Decadal variability of precipitation over Western North America. J. Climatol. 11 (12), 3148–3166.
Cook, E.R., Peters, K., 1981. The smoothing spline: A new approach to standardizing forest interior tree-ring width series for dendroclimatic studies. Tree-Ring Bull 41, 45–53.
Cook, E.R., Kairiuksktis, L. (Eds.), 1990. Methods of Dendrochronology: Applications in the Environmental Sciences. Kluwer Academic Publishers.
Cook, E., Briffa, K., Shiyatov, S., Mazepa, V., 1990. Tree-ring standardization and growth-trend estimation. In: Cook, E.R., Kairiukstis, L. (Eds.), Dendrochronology Applications in the Environmental Sciences. Kluwer Academic Publishers, pp. 178–185.
Cook, E.R., Woodhouse, C.A., Eakin, C.M., Meko, D.M., Stahle, D.W., 2004. Long-term aridity changes in the Western United States. Science 306 (5698), 1015–1018.
Dettinger, M.D., Cayan, D.R., Diaz, H.F., Meko, D.M., 1998. North–South precipitation patterns in Western North America on interannual-to-decadal timescales. J. Climatol. 11, 3095–3111.
Earle, C.J., 1993. Asynchronous droughts in California streamflow as reconstructed from tree rings. Quat. Res. 39 (3), 290–299.
Earle, C.J., Fritts, H.C., 1986. Reconstructing Riverflow in the Sacramento Basin since 1560. Laboratory of Tree-Ring Research, University of Arizona, Tucson.
Fritts, H.C., 2001. Tree Rings and Climate, second ed. Blackburn.
Fritts, H.C., Guiot, J., Gordon, G.A., 1990. Validation, methods of dendrochronology: applications in the environmental sciences. In: Cook, E.R., Kairiukstis, L. (Eds.), Dendrochronology Applications in the Environmental Sciences. Kluwer Academic Publishers, pp. 178–185.
Gedalof, Z., Peterson, D.L., Mantua, N.J., 2004. Columbia River flow and drought since 1750. J. Am. Water Resour. 40 (6), 1579–1592.
Graumlich, L.J., 1993. A 1000-year record of temperature and precipitation in the Sierra Nevada. Quat. Res. 39 (2), 249–255.
Graumlich, L.J., Pisaric, M.F.J., Waggoner, L.A., Littell, J.S., King, J.C., 2003. Upper Yellowstone river flow and teleconnections with pacific basin climate variability during the past three centuries. Clim. Change 59 (1), 245–262.
Haston, L., Michaelsen, J., 1997. Spatial and temporal variability of Southern California precipitation over the last 400 yr and relationships to atmospheric circulation patterns. J. Climatol. 10 (8), 1836–1852.
Holmes, R., 1983. Computer assisted quality control in tree-ring standardization. Tree-Ring Bull. 43, 69–75.
Hughes, M., Funkhouser, G., 1998. Extremes of moisture availability reconstructed from tree rings for recent millennia in the great basin of western north America. In: Beniston, M., Innes, J. (Eds.), The Impacts of Climate Variability on Forests. Lecture Notes in Earth Sciences. Springer, Berlin/Heidelberg, pp. 99–107.
Jain, S., Woodhouse, C.A., Hoerling, M.P., 2002. Multidecadal streamflow regimes in the interior western United States: implications for the vulnerability of water resources. Geophys. Res. Lett. 29. http://dx.doi.org/10.1029/2001GL014278.
Levy, S., 2003. Turbulence in the Klamath River Basin. BioScience 53 (4), 315–320.
Meko, D.M., Woodhouse, C.A., 2005. Tree-ring footprint of joint hydrologic drought in Sacramento and Upper Colorado river basins, western USA. J. Hydrol. 308 (1–4), 196–213.
Meko, D.M., Therrell, M.D., Baisan, C.H., Hughes, M.K., 2001. Sacramento River flow reconstructed to A.D. 869 from tree rings. J. Am. Water Resour. 37 (4), 1029–1039.
Meko, D.M. et al., 2007. Medieval drought in the upper Colorado River Basin. Geophys. Res. Lett. 34 (10).
Meko, D.M., Stahle, D.W., Griffin, D., Knight, T.A., 2011. Inferring precipitation-anomaly gradients from tree rings. Quat. Int. 235 (1–2), 89–100.
Meko, D.M., Woodhouse, C.A., Morino, K., 2012. Dendrochronology and links to streamflow. J. Hydrol. 412–413, 200–209.
Pederson, G.T. et al., 2011. The unusual nature of recent snowpack declines in the North American Cordillera. Science 333 (6040), 332–335.
R Development Core Team, 2012. R: A language and environment for statistical computing. R Foundation for Statistical Computing, Vienna, Austria.
Redmond, K.T., Koch, R.W., 1991. Surface climate and streamflow variability in the Western United States and their relationship to large-scale circulation indices. Water Resour. Res. 27 (9), 2381–2399.
Risley, J.C., Gannett, M.W., Lea, J.K., Roehl Jr, E.A., 2005. An Analysis of Statistical Methods for Seasonal Flow Forecasting in the Upper Klamath River Basin of Oregon and California, US Geological Survey.
Salzer, M.W., Kipfmueller, K.F., 2005. Reconstructed temperature and precipitation on a millennial timescale from tree-rings In The Southern Colorado Plateau, USA. Clim. Change 70 (3), 465–487.
Service, R.F., 2003. 'Combat Biology' on the Klamath. Science 300 (5616), 36–39.
Stahle, D.W. et al., 2000. Tree-ring data documenting the 16th century megadrought over North America. Eos 81 (12), 121–125.
Stahle, D.W. et al., 2001. Ancient blue oaks reveal human impact on San Francisco Bay salinity. Eos 82 (12), 141–145.
Stine, S., 1994. Extreme and persistent drought in California and Patagonia during mediaeval time. Nature 369 (6481), 546–549. http://dx.doi.org/10.1038/369546a0.
Stockton, C.W., Jacoby, G.C., 1976. Long-term Surface-Water Supply and Streamflow Trends in the Upper Colorado River Basin. National Science Foundation, Arlington, VA.
Stokes, M.A., Smiley, T.L., 1996. An Introduction to Tree-Ring Dating. University of Arizona Press, Tucson.
Touchan, R., 1999. A 396-year reconstruction of precipitation in Southern Jordan. J. Am. Water Resour. 35 (1), 49–60.
Touchan, R., Woodhouse, C.A., Meko, D.M., Craig, A., 2011. Millennial precipitation reconstruction for the Jemez Mountains, New Mexico, reveals changing drought signal. Int. J. Climatol 31 (6), 896–906.
US Bureau of Reclamation, 2004. Undepleted natural flow of the Upper Klamath River: natural inflow to natural losses from, and natural outfall of Upper Klamath Lake to the Link River and of Lower Klamath Lake to the Klamath River. Klamath Falls, Or.: US Dept. of the Interior, US Bureau of Reclamation, Klamath Basin Area Office, Klamath Falls, OR.
US Department of the Interior, 2010. Secretary Salazar, Governors Kulongoski and Schwarzenegger Announce Agreement on Klamath River Basin Restoration. <http://www.doi.gov/news/pressreleases/2010_02_18_release.cfm>.
Wallace, J.M., Gutzler, D.S., 1981. Teleconnections in the geopotential height field during the Northern Hemisphere winter. Mon. Weather Rev. 109 (4), 784–812.

Wigley, T.M.L., Briffa, K.R., Jones, P.D., 1984. On the average value of correlated time series, with applications in dendroclimatology and hydrometeorology. J. Clim. Appl. Meteorol. 23 (2), 201–213.
Wise, E.K., 2010. Spatiotemporal variability of the precipitation dipole transition zone in the western United States. Geophys. Res. Lett. 37, L07706.
Woodhouse, C.A., 2003. A 431-yr reconstruction of Western Colorado snowpack from tree rings. J. Climatol. 16 (10), 1551–1561.
Woodhouse, C.A., Russell, J.L., Cook, E.R., 2009. Two modes of North American drought from instrumental and paleoclimatic data. J. Climatol. 22 (16), 4336–4347.